

Is indium tin oxide a suitable electrode in organic solar cells? Photovoltaic properties of interfaces in organic *p/n* junction photodiodes

Woong Sang Jahng and Anthony H. Francis

Department of Chemistry, The University of Michigan, Ann Arbor, Michigan 48109-1055

Hyunsik Moon and John I. Nanos

Macromolecular Science & Engineering Center, The University of Michigan, Ann Arbor, Michigan 48109-1055

M. David Curtis^{a)}

Department of Chemistry, and the Macromolecular Science & Engineering Center, The University of Michigan, Ann Arbor, Michigan 48109-1055

(Received 31 August 2005; accepted 17 January 2006; published online 27 February 2006)

The charge generation properties at all interfaces of a *p/n* junction, bilayer photodiode have been investigated by means of the photoaction spectrum (PAS) as a function of applied bias. The organic photodiode was fabricated with a low-glass transition temperature (T_g) polysiloxane with pendant hydrazone groups as the *p*-type material and a perylene diimide derivative as the *n*-type material. The PAS under short circuit and reverse bias showed an antibatic response at the high-energy region (3.0–3.5 eV), and a symbatic response at the low-energy region (2.0–3.0 eV). However, under forward bias, the PAS showed the opposite behavior. These results are interpreted in terms of the band structure of tin-doped indium oxide (ITO) that prevents effective photoinjection of electrons at the polymer/ITO interface and the relative energy levels of the constituent materials. © 2006 American Institute of Physics. [DOI: 10.1063/1.2180881]

Bulk heterojunction solar cells and *p/n* junction photodiodes possess high potential for use in many consumer applications because charge separation is enhanced by the potential energy differences at the interfaces.^{1–5} Many researchers have focused on indium tin oxide (ITO) as the transparent electrode in such solar cells, as well as in other applications that require high conductivity and transparency in the visible spectrum, e.g., organic light emitting diodes (OLEDs).^{6–10} The photoaction spectra of a photodiode as a function of applied bias provides valuable information from which both the charge generation sites and the main carrier species may be deduced.^{11–15}

In this letter, the current density-voltage (*J-V*) characteristics and the photoaction spectra have been used to investigate charge generation and transport properties of bilayer, *p/n* junction photodiodes as these relate to the performance of the ITO electrode.

The photocells were fabricated from hydrazone-substituted polysiloxane, poly[methyl-(*N*-propyl-*N*-(4-diphenylhydrazono-methylphenyl)amino)siloxane (PSX-Hz) as the *p*-type material, and a perylenediimide derivative, 1, 2-diaminobenzene perylene-3,4,9,10-tetracarboxylic acid diimide (PV) as the *n*-type material (see Fig. 1). PSX-Hz has a low glass transition temperature (softens at a low temperature) and was chosen as a cell component in order to investigate the possibility of fabricating bilayer solar cells via a simple lamination procedure. The lamination results will be reported separately.

PSX-Hz was synthesized according to the literature.¹⁶ Uniform films (100 nm thickness) of PSX-Hz were deposited onto patterned, oxygen-plasma-etched ITO glass by spincoating. PV (50 nm) was vacuum-deposited at

2×10^{-6} Torr on top of the polysiloxane films. The effective areas of the devices were 0.09 cm². Bismuth was selected as the back electrode to take advantage of its oxidative stability and suitable workfunction, $\phi_{\text{Bi}}=4.22$ eV. The energy levels of the cell materials, PV: Highest occupied molecular orbital (HOMO)=6.0 eV, lowest unoccupied molecular orbital (LUMO)=2.5 eV, and PSX-Hz: HOMO=5.3 eV, LUMO=2.3 eV, were estimated from the absorption edges of the ultraviolet-visible spectra and the oxidation potentials as obtained from cyclic voltametry. The bilayer, *p/n* junction photodiode, ITO/PSX-Hz(100 nm)/PV(50 nm)/Bi(50 nm) was used to obtain the results presented in this letter.

Figure 1 displays the *J-V* curves of a typical ITO/PSX-Hz/PV/Bi device. The monochromatic power conversion efficiency was 0.1% at 550 nm, ($10 \mu\text{W}/\text{cm}^2$, $V_{\text{oc}}=0.31$ V, $J_{\text{sc}}=0.18 \mu\text{A}/\text{cm}^2$, FF (fill factor)=0.34). The absorption

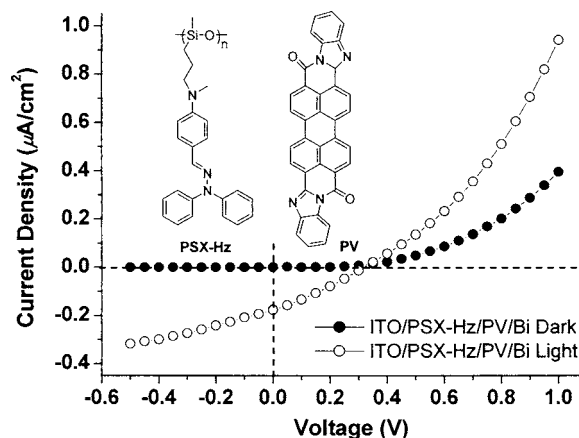


FIG. 1. *J-V* curves of the device, ITO/PSX-Hz/PV/Bi, in the dark (filled) and under 550 nm illumination (open). The insets show the chemical structure of PSX-Hz and PV.

^{a)}Electronic mail: mdcurtis@umich.edu

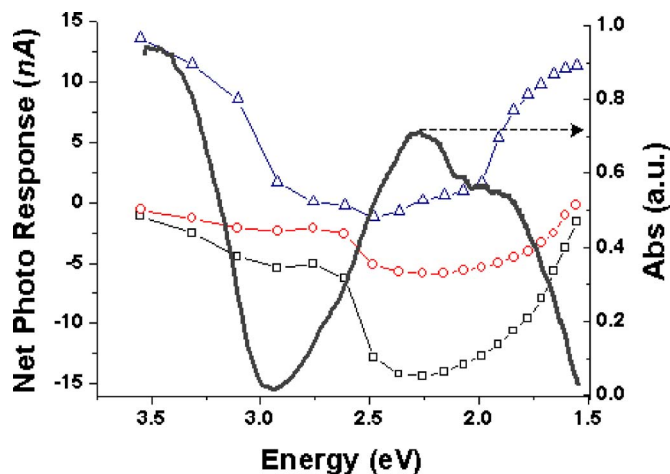


FIG. 2. (Color online) Photoaction spectra of ITO/PSX-Hz/PV/Bi under short circuit (0 V; open circles), forward bias (+1.0 V; triangles) and reverse bias (-1.0 V; squares). The normalized absorption spectrum is also shown (heavy line).

spectrum, and the photoaction spectra of the photocell (illuminated through the ITO electrode) under short circuit, forward and reverse biases are shown in Fig. 2. The net photocurrent responses have been corrected for the light intensities of the Xe lamp at the different wavelengths. The absorption above 3.0 eV is due to the PSX-Hz, and the absorption below 3.0 eV is due to the PV. Under short circuit, the photocell showed a negative photocurrent (circles on Fig. 2), i.e., electrons move through the device toward the Bi electrode due to the built-in electric field that results from the difference in workfunctions of the ITO and Bi electrodes. A reverse bias reinforces the built-in field, so that the action spectrum under -1.0 V has the same shape as the action spectrum under zero applied voltage, but the photocurrent is increased (Fig. 2).⁵

Although light in the region 3.0–3.5 eV causes some photocurrent, the response to these energies is weak, and the photoresponse would be classified as antibatic (does not parallel the absorption spectrum) in this region. Conversely, the photoresponse is symbatic (parallel to the absorption spectrum) in the region where PV absorbs (1.75–2.75 eV). This type of behavior has been described before and arises when the *p/n* interface is the primary locus of charge generation.³ Due to the high absorption coefficient of the PSX-Hz, most photons in the energy region, 2.8–3.0 eV, are absorbed by the PSX-Hz and do not reach the *p/n* interface where charge separation occurs. Light that is absorbed some distance (≥ 10 nm) from the interface is not effective for charge generation because of the limited exciton diffusion distance. However, the low-energy light (2.0–2.5 eV) is strongly absorbed by the PV, with the greatest rate of exciton generation occurring near the *p/n* interface. These Frenkel excitons are represented in Fig. 3(a) as a hole in the valence band ($E_v \approx E_{\text{HOMO}}$) and an electron in the conduction band ($E_c \approx E_{\text{LUMO}}$) of the PV. Because of the favorable energy offsets of the respective HOMOs and LUMOs of PSX-Hz and PV, the exciton is dissociated, with the hole being transferred to the PSX-Hz, and the electron to the PV. Under the built-in bias or a negative applied bias, the holes are accelerated toward the ITO and the electrons toward the Bi electrode, giving the observed symbatic photoresponse (Fig. 2).

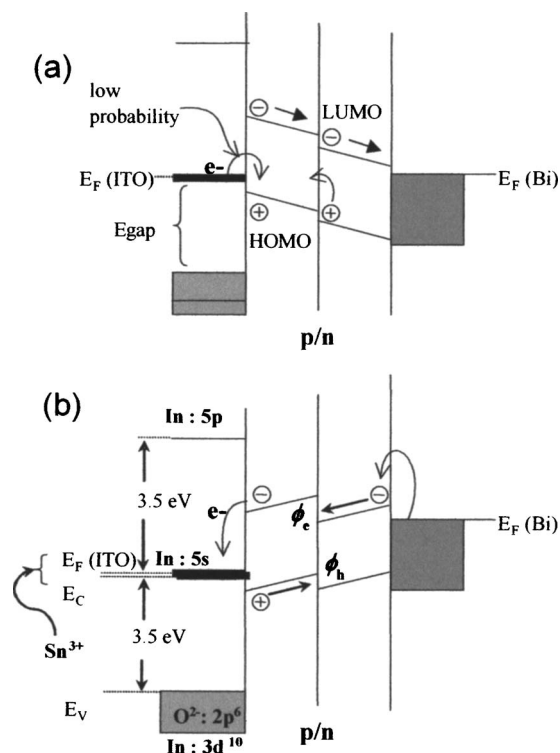


FIG. 3. Schematic energy band structure at short circuit (a) and under forward bias (b) of the ITO/PSX-Hz/PV/Bi photocell. The energy levels for ITO represent the calculated energy-band model for Sn-doped In_2O_3 (ITO, see Ref. 18).

The lack of a photoresponse to photon energies near 3.5 eV indicates that the excitons generated in the PSX-Hz near the ITO interface are *not* effective for charge generation. This observation has been made before, and the poor efficiency was ascribed to the decay of electron carriers in the polymer layer.¹⁷ We believe that ITO is intrinsically inefficient for photoinjection of electrons due to its band structure; and we describe two possible mechanisms for the lack of effective charge generation near the ITO interface. Both mechanisms are based on the low density of filled states near the Fermi level of the ITO. The workfunction of ITO ($\phi_{\text{ITO}}, 4.8$ eV) is well matched to the HOMO energy of PSX-Hz and a large number of other hole transporting organic materials [Fig. 3(a)]. However, there is an important difference between ITO and a metal electrode: ITO consists of Sn-doped (*n*-doped) In_2O_3 , an intrinsic insulator. Even as an *n*-doped conductor, ITO still has a wide band gap from 3.50 to 4.06 eV, i.e., just below the sparsely populated conduction band.¹⁸ The low density of electrons in the conduction band leads to low rate of combination with the holes of the photogenerated electron-hole pairs in the PSX-Hz adjacent to the ITO/PSX-Hz interface. (This recombination may be approximated as a second order reaction, $\text{rate} = k[h^+][e^-]$.) A rate of electron transfer from the ITO to PSX-Hz that is less than the rate of exciton hole-electron recombination promotes decay of the excitons without charge generation. The completely filled valence band of ITO does not contribute to the charge separation process because the top of the ITO valence band lies more than 3.0 eV below the HOMO of PSX-Hz.

An alternate mechanism allows for a rapid transfer of an electron from the conduction band of ITO to the hole in the HOMO of PSX-Hz with the concomitant generation of a

hole in the ITO conduction band spatially proximate to the electron in the LUMO of the polymer. In this mechanism, the transfer of the electron from the LUMO of PV to the hole in the ITO is very rapid due to the high density of empty states in the ITO valence band and the favorable energetics. In this mechanism, the PSX-Hz exciton is rapidly quenched at the ITO interface via charge transfer, but without net charge generation. In either mechanism, the lack of charge generation is due to the ITO band structure, in particular, the large energy gap just below the Fermi level.

On the other hand, the photoaction spectrum is symbatic with respect to the absorption spectrum of PSX-Hz under a forward bias sufficiently large to overcome the built-in field (Fig. 2). Under these conditions, electron-hole pairs photo-generated in the PSX-Hz near the ITO surface can inject an electron into the conduction band of ITO, leaving behind a hole that is accelerated toward the back electrode by the applied field [Fig. 3(b)]. As in the second mechanism proposed above, the injection of an electron from the LUMO of PSX-Hz occurs with high probability.

Moreover, the PAS also shows that the *p/n* interface is not effective in charge separation under forward bias. Holes traveling from the PSX-Hz to the PV, and electrons traveling from PV to PSX-Hz face energy barriers, φ_h and φ_e , respectively [Fig. 3(b)], at the *p/n* interface, leading to a higher probability of carrier recombination. The photoresponse does increase at low photon energies (≤ 2.0 eV) in the region where neither the PSX-Hz nor the PV absorbs. Light with these energies strikes the Bi electrode, causing photoinjection of electrons that tunnel through the barrier at the *p/n* interface.

The poor electron injection from ITO means that the blue end of the visible spectrum is not effective in generating photocurrent in organic solar cells with ITO front electrodes. A thin coating of metal, e.g., gold, on the ITO improves performance by restoring a symbatic photoresponse at high

energies,¹⁹ as does coating the ITO with PEDOT/PSS, a polymeric conductor.²⁰

The authors are grateful to TouchSensor Technologies, LLC; the Petroleum Research Fund, administered by the American Chemical Society; and The Research Corporation for support of this research.

¹B. O'Regan and M. Grätzel, *Nature (London)* **353**, 737 (1991).

²C. W. Tang, *Appl. Phys. Lett.* **48**, 183 (1986).

³G. Yu, J. Gao, J. C. Hummelen, F. Wudl, and A. J. Heeger, *Science* **270**, 1789 (1995).

⁴J. J. M. Halls, C. A. Walsh, N. C. Greenham, E. A. Marseglia, R. H. Friend, S. C. Moratti, and A. B. Holmes, *Nature (London)* **376**, 498 (1995).

⁵J. Xue, S. Uchida, B. P. Rand, and S. R. Forrest, *Appl. Phys. Lett.* **85**, 5757 (2004).

⁶R. F. Service, *Science* **273**, 1789 (1995).

⁷W.-L. Yu, J. Pei, W. Huang, and A. J. Heeger, *Chem. Commun. (Cambridge)*, 1837 (1999).

⁸B. Tsuie, J. L. Reddinger, G. A. Sotzing, J. Soloducho, A. R. Katritzky, and J. R. Reynolds, *J. Mater. Chem.* **9**, 2189 (1999).

⁹X.-C. Li, Y. Liu, M. S. Liu, and A. K.-Y. Jen, *Chem. Mater.* **11**, 1568 (1999).

¹⁰A. Dodabalapur, E. A. Chandross, M. Berggren, and R. E. Slusher, *Science* **277**, 1787 (1997).

¹¹M. G. Harrison, J. Grüner, and G. C. W. Spencer, *Phys. Rev. B* **55**, 7831 (1998).

¹²R. N. Marks, J. J. M. Halls, D. D. C. Bradely, R. H. Friend, and A. B. Holmes, *J. Phys.: Condens. Matter* **6**, 1379 (1994).

¹³A. J. Breeze, A. Salomon, D. S. Ginley, H. Tillmann, H.-H. Hörhold, and B. A. Gregg, *Appl. Phys. Lett.* **81**, 3085 (2002).

¹⁴L. Tan, M. D. Curtis, and A. H. Francis, *Macromolecules* **35**, 4628 (2002).

¹⁵L. Tan, M. D. Curtis, and A. H. Francis, *Chem. Mater.* **15**, 2272 (2003).

¹⁶S. H. Lee, W. S. Jahng, K. H. Park, N. Kim, W. Joo, and D. H. Choi, *Macromol. Res.* **11**, 431 (2003).

¹⁷A. C. Arias, N. Granström, K. Petrisch, and R. H. Friend, *Synth. Met.* **102**, 953 (1999).

¹⁸J. C. C. Fan and J. B. Goodenough, *J. Appl. Phys.* **48**, 3524 (1977).

¹⁹W. S. Jahng and M. D. Curtis (unpublished).

²⁰F. Zhang, M. Johansson, M. R. Andersson, J. C. Hummelen, and O. Inganäs, *Adv. Mater. (Weinheim, Ger.)* **14**, 662 (2002).